

Characterization of Six Isomers of [84]Fullerene C₈₄ by Electrochemistry, Electron Spin Resonance Spectroscopy, and Molecular Energy Levels Calculations

José Antonio Azamar-Barríos,[†] T. John S. Dennis,^{‡,§} Shaumo Sadhukan,^{||} Hisanori Shinohara,[‡] Gustavo E. Scuseria,^{||} and Alain Pénicaud^{*,⊥}

Departamento de Física aplicada, CINVESTAV-IPN-Mérida, apdo postal 73 Cordemex, 97310 Mérida,

Yuc., México, Department of Chemistry, Nagoya University, Nagoya 464-8602, Japan,

Department of Chemistry and Rice Quantum Institute, Rice University, Houston, Texas 77251-1892, and Centre de Recherche Paul Pascal, CNRS (UPR8641), Université de Bordeaux-I, av. Schweitzer, 33600 Pessac, France

Received: October 5, 2000; In Final Form: February 19, 2001

The electrochemical and electron spin resonance (ESR) fingerprints of six isomers of C₈₄ [*D*₂(IV), *D*_{2*d*}(II), *D*_{2*d*}(I), *D*₂(II), *C*₂(IV), and *C*_s(b)] are presented together with density functional theory (DFT) calculations of the molecular orbitals (MO) energy levels for a total of 10 isomers (*D*₂(IV), *D*_{2*d*}(II), *D*_{2*d*}(I), *D*₂(II), *C*_s(V), and *C*₂(I) to *C*₂(V)). Comparison between calculations and electrochemical data shows a true synergy between calculated energy levels and experimental redox potentials. Assignments are proposed of the *C*₂ isomer as *C*₂(IV) and tentatively of the *C*_s(b) isomer as *C*_s(V). The temperature-dependent ESR spectra of *D*₂(IV) and *D*_{2*d*}(II) singly charged ions show an abrupt change around 150 K which is ascribed to a change of spin state. Additionally, the room-temperature solution ESR spectra of all isomers studied exhibit a fine structure characteristic of each isomer.

1. Introduction

In the past eight years, higher fullerenes chemistry and physical chemistry have developed at a steady pace, albeit slower than that of their main counterparts C₆₀ and C₇₀, owing to limited quantities available. It has been known for some time that C₈₄ consists mainly of a mixture of two isomers noted *D*₂(IV) and *D*_{2*d*}(II),^{1,2} which were recently separated by HPLC.³ They have been electrochemically characterized,^{4–8} and their radical anions have been studied by ESR spectroscopy.^{5,7} Additionally, [84]fulleride salts of those two isomers have been synthesized by doping with potassium vapor⁹ while some years ago [84]*D*_{2*d*}(II) was isolated in η²-C₈₄IrCOCl(PPh₃)₂ whose crystal structure was solved by X-ray diffraction.¹⁰ The crystal structure of the mixture of the two main C₈₄ isomers has also been recently determined¹¹ and their infrared spectra reported as a function of temperature.¹² From the beginning, it has been known that there were also additional minor isomers.^{2b} From the ³He NMR spectra of the He@C₈₄ mixture, the presence of eight isomers was suggested¹³ and a first attempt at their identification was made in 1997.¹⁴ Recently, some of us succeeded in isolating in milligram quantities and identifying (by ¹³C NMR spectroscopy) five additional minor isomers of C₈₄ (*C*₂, *C*_s(a), *C*_s(b), *D*_{2*d*}(I), and *D*₂(II) in order of decreasing abundance).¹⁵ Using another preparation route, two other isomers of *D*_{3*d*} and *D*_{6*h*} symmetry were also isolated,¹⁶ whereas an elegant, reversible, functionalization of the C₈₄ mixture allowed the separation of the two main isomers plus an, as yet unidentified, third minor isomer.¹⁷ Now that [84]fullerene begins

to exist as purified isomers, it is important to characterize them by electrochemistry which has proven in the past to be an invaluable analysis and identification tool for fullerenes. Furthermore, taking advantage of the computing power now available, it is possible to confront electrochemical data with accurate energy levels calculations. Using a recently reported electrochemical setup,⁷ we have performed cyclic voltammetry experiments of six C₈₄ isomers (i.e., the two major ones and the *C*₂, *C*_s(b), *D*_{2*d*}(I), and *D*₂(II) minor isomers) and prepare their singly reduced radical anions. We report their electrochemical characterization in benzonitrile and 1,1,2,2-tetrachloroethane (TCE) and the ESR characterization of their radical anions. Additionally, molecular orbitals (MO) energy levels calculations were performed using density functional theory (DFT) and compared with the electrochemical data. Comparison between calculations and electrochemical data shows a remarkable synergy between calculated energy levels and experimental redox potentials, reinforcing the earlier NMR-based assignment¹⁵ for four of the isomers under study. Moreover, plots of the energy levels vs the electrochemical redox potentials allowed the identification of isomer *C*₂ as *C*₂(IV) and tentative identification of *C*_s(b) as *C*_s(V). Basic characterization (*g*-value, line width) of the six singly charged isomeric anions was performed after full electrolysis of each isomer solution. The ESR study showed temperature-dependent ESR spectra for the *D*₂(IV) and *D*_{2*d*}(II) singly charged ions with an abrupt change around 150 K which is ascribed to a change of spin state. After warming up to room temperature, the solution ESR spectra of all isomers studied exhibit a fine structure, characteristic of each isomer.

2. Experimental Section

Isolation and identification of the different isomers have been reported previously.^{3,15} Cyclic voltammograms were obtained under inert atmosphere conditions following a procedure already described.⁷ The reference electrode was Ag/Ag⁺. All potentials

* Author to whom correspondence should be addressed. Fax: (33)5 56 84 56 00. E-mail: Penicaud@crpp.u-bordeaux.fr.

[†] CINVESTAV-IPN-Mérida.

[‡] Nagoya University.

[§] Present address: Department of Chemistry, Queen Mary, University of London, London E1 4NS, U.K.

^{||} Rice University.

[⊥] Université de Bordeaux-I.

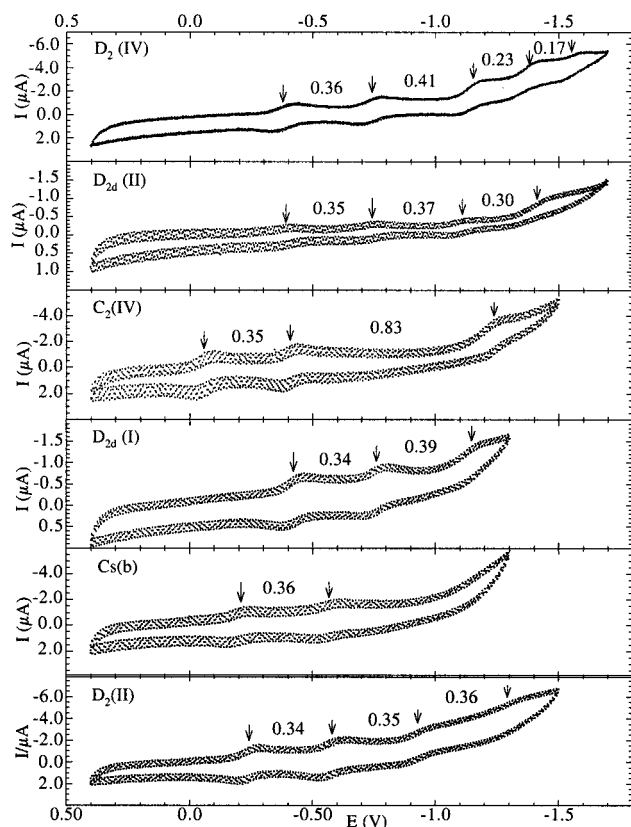


Figure 1. Cyclic voltammograms in benzonitrile, 0.05 M PPNCl (PPN = $[(C_6H_5)_3P]_2N^+$), reference: Ag/Ag^+ ($E_{1/2}[Fc/Fc^+] = +0.22$ V vs Ag/Ag^+). Scan rate: 100 mV/s. Arrows indicate approximate $E_{1/2}$ values. Numbers between the arrows express potential differences (volts).

are referred to ferrocene measured under identical conditions ($E_{1/2}[Fc/Fc^+] = +0.22$ V vs Ag/Ag^+). Full electrolysis of each isomer solution was performed at a constant potential slightly higher than the first reduction potential and the electrolyzed solution was vacuum transferred to an ESR tube which was sealed and kept at liquid nitrogen temperature while waiting for the ESR measurements to be performed. ESR measurements were performed on a Bruker X-band spectrometer equipped with a double cavity and an Oxford ESR900 cryostat. Molecular orbitals calculations: atomic coordinates were taken from the web site (<http://shachi.cochem2.tutkie.tut.ac.jp/Fuller/higher/higherE.html>). After further geometry optimization (AM1) of each isomer, MO energy calculations were performed with Gaussian using LSDA/3-21G, LSDA/6-31G*, BLYP/3-21G, and BLYP/6-31G*.

3. Results and Discussion

Electrochemistry/Molecular Orbital Energy Calculations.

Cyclic voltammograms in benzonitrile and 1,1,2,2-tetrachloroethane (TCE) for all six isomers are presented in Figures 1 and 2, while the redox potentials in benzonitrile and TCE are summarized in Tables 1 and 2. In benzonitrile, up to 5 reduction waves can be seen for $D_2(IV)$, 4 for $D_{2d}(II)$, 3 for $C_2(IV)$, 3 for $D_{2d}(I)$, 2 for $C_s(b)$, and 4 for $D_2(II)$. In TCE, reversible oxidation peaks were detected for four of the isomers under study (reversible is here used in the loose sense of the existence of an opposite peak when the scan is reversed). No quantitative study of the degree of reversibility of those oxidation peaks has been performed).

Calculations were made using density functional theory (DFT) with bases including (6-31G*) or excluding (3-21G) d-orbitals

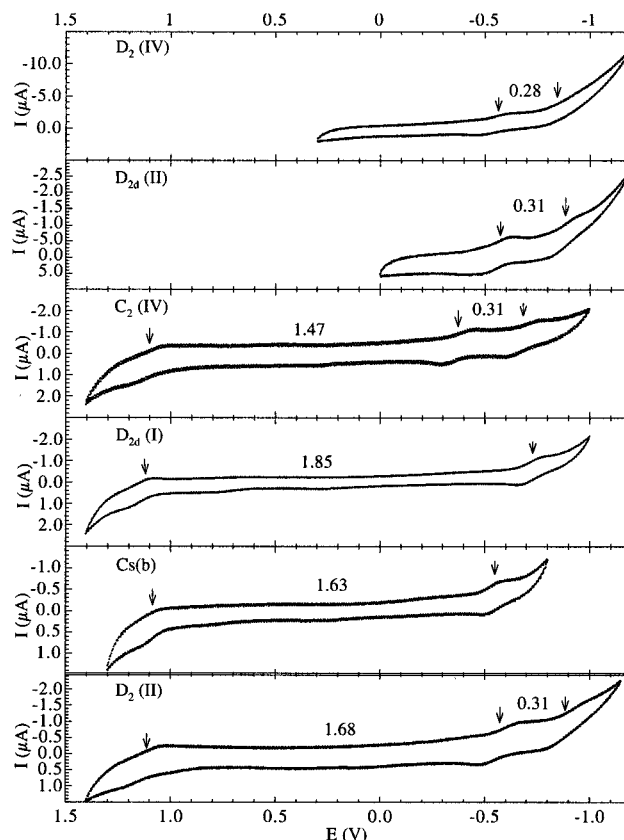


Figure 2. Cyclic voltammograms in TCE, 0.05 M $Bu_4N.PF_6$, reference: Ag/Ag^+ ($E_{1/2}[Fc/Fc^+] = +0.22$ V vs Ag/Ag^+). Scan rate: 100 mV/s. Arrows indicate approximate $E_{1/2}$ values. Numbers between the arrows express potential differences (volts).

TABLE 1: Half-Wave Potentials (volts, referenced to Fc/Fc^+ , $E[Fc/Fc^+] = +0.22$ V vs Ag/Ag^+) and Peak-to-Peak Potential Differences (volts, in parentheses) in Benzonitrile, 0.05 M PPNCl (PPN = $[(C_6H_5)_3P]_2N^+$)

isomer	0/-1	-1/-2	-2/-3	-3/-4	-4/-5
$D_2(IV)$	-0.60(0.08)	-0.96(0.06)	-1.37(0.11)	-1.60(0.12)	-1.77(0.08)
$D_{2d}(II)$	-0.61(0.05)	-0.96(0.05)	-1.33(0.07)	-1.63(0.13)	
$C_2(IV)$	-0.28(0.06)	-0.63(0.05)	-1.46(0.04)		
$D_{2d}(I)$	-0.64(0.06)	-0.98(0.06)	-1.37(0.08)		
$C_s(b)$	-0.43(0.05)	-0.79(0.05)			
$D_2(II)$	-0.46(0.06)	-0.80(0.08)	-1.15(0.10)	-1.51(0.08)	

TABLE 2: Half-Wave Potentials (volts, referenced to Fc/Fc^+ , $E[Fc/Fc^+] = +0.22$ V vs Ag/Ag^+), Peak-to-Peak Potential Differences (volts, in parentheses), and Electrochemical Window ($E_{ox} - E_{red}$) in 1,1,2,2-Tetrachloroethane, 0.05 M $Bu_4N^+PF_6^-$

isomer	+1/0	0/-1	-1/-2	$E_{ox} - E_{red}$
$D_2(IV)$		-0.78(0.13)	-1.06(0.09)	
$D_{2d}(II)$		-0.79(0.11)	-1.10(0.13)	
$C_2(IV)$	0.88(0.14)	-0.59(0.14)	-0.90(0.14)	1.47
$D_{2d}(I)$	0.91(0.10)	-0.94(0.08)		1.85
$C_s(b)$	0.86(0.08)	-0.77(0.07)		1.63
$D_2(II)$	0.89(0.16)	-0.79(0.17)	-1.10(0.17)	1.68

and yielded slightly different absolute values for the MO energies but similar energy differences. Both LSDA and BLYP methods yielded the same results for a given basis set. Hence, in the rest of the paper, we will use the results of only one type of calculations per isomer. For sake of completeness, we use the BLYP (6-31G*) results albeit one has to bear in mind that the results were not dependent on the method or the basis set used. Energy levels for the six isomers under study are plotted in Figure 3.

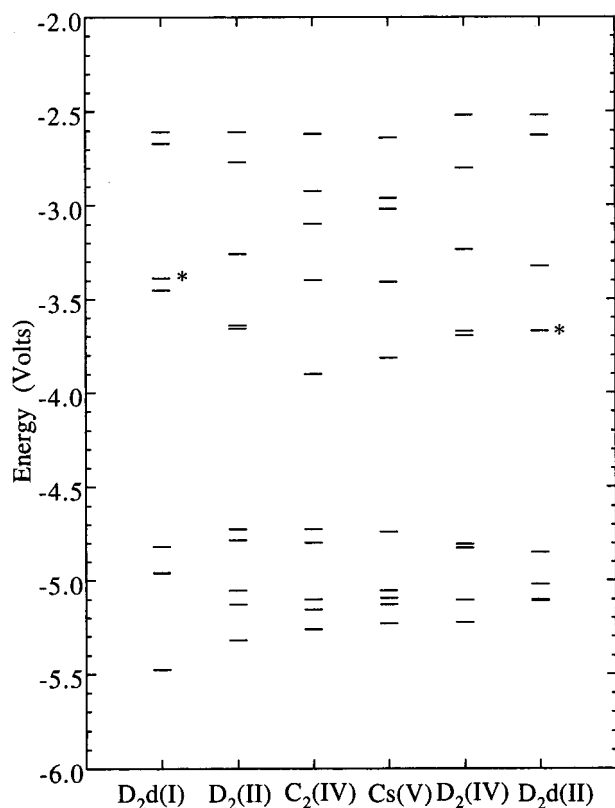


Figure 3. Molecular orbitals energy levels obtained by DFT calculations (see text). (*) denotes doubly degenerate levels.

The following points are noteworthy:

(i) The voltammograms of the two major isomers ($D_2(IV)$ and $D_{2d}(II)$) are undistinguishable up to the third reduction wave. This is to be expected from their very similar MO diagram: $D_{2d}(II)$ has a degenerate LUMO, while $D_2(IV)$ LUMO and LUMO+1 levels are very close in energy (0.00084 hartrees).

(ii) The first reduction wave of [84] $C_2(IV)$ is situated at strikingly less negative potentials, i.e., $C_2(IV)$ is easier to reduce, than the other C_{84} isomers (and the other fullerenes as well). This correlates very well with it having the lowest LUMO among all studied C_{84} isomers (Figure 3). This is the first member of the fullerene family to approach (by 60 mV) the reduction potential of TCNQ (tetracyanoquinodimethane).¹⁸ Thus, if higher fullerenes are available in larger quantities in the future, charge-transfer salts should be obtainable between TTF (or substituted TTF's, TTF = tetrathiafulvalene) and [84]- $C_2(IV)$.¹⁹

(iii) For all six isomers, reduction waves are shifted toward more negative potentials in TCE but the overall scans are similar. This is added evidence to the growing list of significant solvent–fullerene interactions.^{7,20–22}

(iv) All C_{84} isomers can be reversibly oxidized as is the case of the lighter fullerenes⁶: In TCE, we were able to detect oxidation waves for the 4 minor isomers studied, the two major ones having already been reported to present an oxidation wave (as an isomer mixture) at a potential slightly outside our electrochemical window.⁶

(v) The overall agreement between the DFT calculations and the observed redox potentials is striking. There is a good linear correlation between the electrochemical redox potentials and the calculated energy levels as well as between the electrochemical window (i.e., the difference between the first reduction potential and the first oxidation potential) and the calculated HOMO-LUMO gaps (Figure 4). One should not expect a perfect

linear relationship since the calculations concern gas-phase isolated neutral molecules at $T = 0$ K while the electrochemical gap will also be function of solvation energies, ion pairing energies, and so on. Echegoyen et al. already observed such a correlation for C_{60} , C_{70} , C_{76} , and C_{78} , using Hartree–Fock data, albeit with overestimated HOMO–LUMO gaps.⁶ It is noteworthy that, when converting the DFT based results from hartrees to volts, one obtains the right order of magnitude, i.e., the calculated HOMO-LUMO gaps are inferior to the electrochemical windows by ca. 0.5 V. When DFT calculations are available for the other fullerenes (C_{60} , C_{70} ,...) it will be interesting to plot the electrochemical parameters vs energy levels for the whole family.

$C_2(IV)$ and $C_s(b)$ identification: Indeed, taking advantage of the correlations mentioned above, we attempted to identify, from the experimental electrochemical values, the $C_2(IV)$ and $C_s(b)$ isomers. The $C_2(IV)$ isomer was known to belong to the C_2 point group symmetry,¹⁵ which reduced its possible identity to the five IPR (isolated pentagon rule) C_2 isomers. BLYP (6-31G*) DFT calculations were thus performed on all five isomers. The calculated values for all five isomers were then plotted in Figure 4 and compared with the expected values from the linear relationship drawn from the known isomers.²³ Although none of the plots in itself gave an unambiguous answer, since one has to allow for deviation from linearity, each of these plots allowed us to discard one or several possibilities. After taking into accounts all four plots, the only reasonable possibility for the C_2 isomer is $C_2(IV)$. Although, we have not performed the same work on the $C_s(b)$ isomer, it can be seen in Figure 4 that $C_s(V)$ is a good candidate. However, since we do not have calculations for the four other C_s isomers, there remains the possibility that one of them has similar energy levels. Thus, we assigned isomer C_2 as isomer $C_2(IV)$ and tentatively isomer $C_s(b)$ as isomer $C_s(V)$. Indeed, ¹³C NMR data for the $C_s(b)$ isomer are consistent with $C_s(III)$ and $C_s(V)$ only¹⁵ and theoretical calculations indicate that $C_s(V)$ is much more stable than $C_s(III)$ (refs 12–19 of ref 15).

It is noteworthy that these two isomers are the only ones presenting a large gap between their second and third reduction potentials (actually, we did not even observe the third wave for the C_s isomer). This correlates with the fact that they have a large energy difference between their LUMO and their “LUMO + 1” level, unlike the other four isomers.

After reading the report of Echegoyen et al. where they isolated a third, unidentified C_{84} isomer besides the two major ones,¹⁷ we were interested to see if we could identify it with one of the minor isomers that we report here. These authors make the observation that this unidentified isomer also presents a large gap between the second and third reduction potential and they use this argument to suggest that their “third isomer” is the same as one isomer erroneously reported as $D_{2d}(II)$.⁸ When comparing the reductions potentials Echegoyen et al. have obtained for the $D_2(IV)$ and $D_{2d}(II)$ isomers in pyridine with those we have determined for the same isomers in benzonitrile, one observes a slight difference of 0.05 to 0.13 V. Taking this into account, and comparing the electrochemical data of refs 8 and 17 with ours, we can readily discard all isomers studied in this report but for $C_s(b)$ that presents similar first and second reduction potentials. Of course, it is still possible that this unidentified isomer be the $C_s(a)$, D_{3d} or D_{6h} isomer for which there are still no published electrochemical data to the best of our knowledge or even a new isomer.

Electron Spin Resonance. Temperature-dependent electron spin resonance (ESR) experiments were performed on the

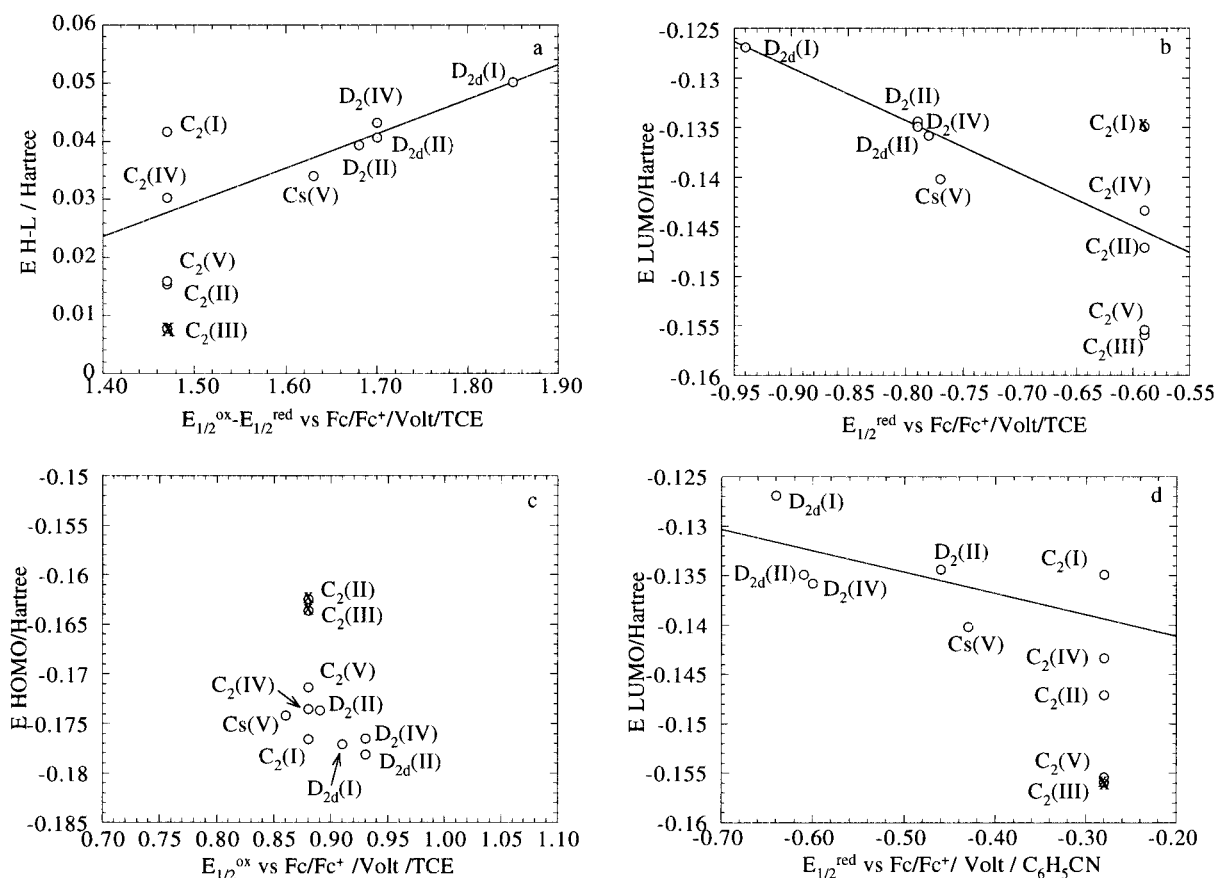


Figure 4. Correlation between calculated energy levels and experimental electrochemical data. For plots a, b, and d, the straight line represents a linear best fit to all isomers²³ but C_2 and C_s (b) (see text). The different calculated entries for the C_2 isomer were used to identify the $C_2(IV)$ isomer (see text). Crossed circles indicate eliminated C_2 candidates. (a) HOMO-LUMO gap vs electrochemical gap in TCE. (b) LUMO energy vs first reduction potential in TCE. (c) HOMO energy vs first oxidation potential in TCE. (d) LUMO energy vs first reduction potential in benzonitrile.

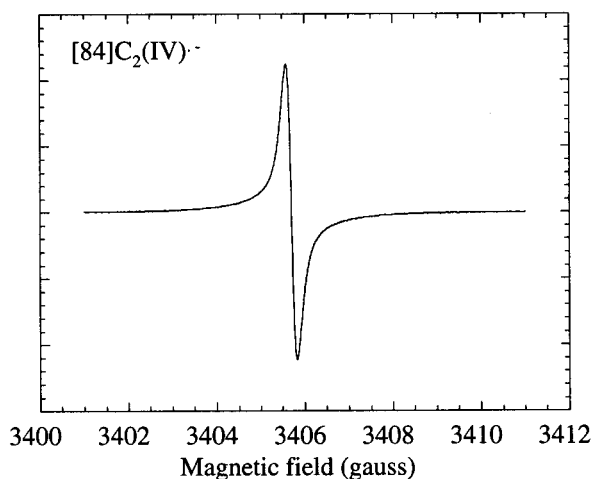


Figure 5. ESR spectrum in frozen benzonitrile at 4 K for $[84]C_2(IV)$ singly charged anion.

solutions of the singly charged anion-radicals in benzonitrile. None of the solutions electrolyzed in TCE, either on the anodic or cathodic side, showed any signal in ESR, probably indicating poor stabilization of the radicals formed in this solvent. All of the isomers under study showed a well-defined isotropic signal with high signal-to-noise ratios (a typical spectrum is shown in Figure 5) but for $D_{2d}(I)$ which exhibited a composite signal albeit with a poor signal-to-noise ratio.

g -values (line widths in gauss) at 4 K in frozen benzonitrile for the monoanions of the $D_2(IV)$, $D_{2d}(II)$, $C_2(IV)$, $D_{2d}(I)$, C_s - (b) and $D_2(II)$ isomers are, respectively, 2.0006 (0.41), 2.0008

(0.39), 2.0006 (0.25), 2.0014 (2.16), 2.0012 (0.43), and 2.0017 (1.00). For the two main isomers $D_2(IV)$ and $D_{2d}(II)$, there are already reported values, obtained on an isomeric mixture by Kadish and co-workers.⁵ Our values are significantly different from their values (2.003 and 2.002, respectively, for $D_2(IV)$ and $D_{2d}(II)$ in pyridine) while they agree with a previous value we have obtained for the isomeric mixture (2.0008). In the absence of other arguments, one may invoke strong solvent interactions to explain that discrepancy.

ESR spectra were recorded as a function of temperature from 4 to 220 K (benzonitrile freezing point). The g -values are constant but for the two main isomers $D_2(IV)$ and $D_{2d}(II)$ (Figure 6). While the line widths for all other isomers are nearly constant as a function of temperature, the line widths of the $D_2(IV)$ and $D_{2d}(II)$ anions also show a dramatic variation (Figure 7). From the energy level calculations, $D_2(IV)$ is known to have a low-lying level close to its LUMO (Figure 3). On the other hand $D_{2d}(II)$ has a degenerate LUMO, but its radical-anion is expected to exhibit a Jahn-Teller distortion that would remove the degeneracy of the occupied level. Hence, in both cases, an excited spin state should be available close in energy to the ground state. In consequence, it was attempted to fit the observed g -value variation with a temperature-dependent population of two different spin states. This is analogous to the case of spin transition systems.²⁴ Let's call 1 and 2 the two different spin states, 1 being the ground state with population $1 - x$ and g -value g_1 and 2 the excited state with population x and g -value g_2 . If the g -values are sufficiently close in energy, i.e., $g_2 - g_1 < \Delta H$, a single signal is expected which g -value will be the weighed average:

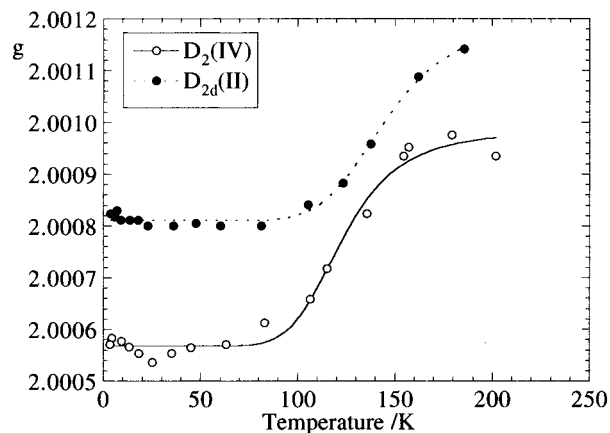


Figure 6. g -value vs temperature for $D_2(\text{IV})$ and $D_{2d}(\text{II})$ singly charged anions.

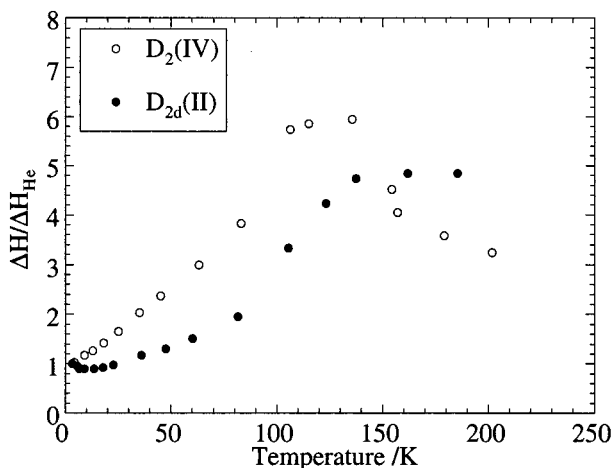


Figure 7. Line widths vs temperature for $D_2(\text{IV})$ and $D_{2d}(\text{II})$ singly charged anions.

$$g = (1 - x)g_1 + xg_2 \Leftrightarrow g = g_1 + x(g_2 - g_1) \quad (1)$$

In the study of spin states transitions in dilute solutions, where no solid-state cooperative effects are expected, but where an entropy term is included, the variation of the population x is expressed as²⁴

$$x = 1/(1 + \exp[(\Delta H/R)(1/T - 1/T_c)]) \quad (2)$$

where ΔH is the enthalpy variation associated with the transformation from spin state 1 to spin state 2, R is the gas constant, and T_c is the temperature for which $x = 0.5$, i.e., both spin states are present in equal amounts. Inserting eq 2 into eq 1 allowed us to fit the experimental data for both isomers (Figure 6). g_1 , g_2 , $\Delta H/R$ (K) and T_c (K) for isomers $D_2(\text{IV})$ and $D_{2d}(\text{II})$ (uncertainty in parentheses) are, respectively, 2.0006 (7×10^{-6}), 2.0010 (3×10^{-5}), 1000 (200), 123 (4), and 2.0008 (3×10^{-6}), 2.0012 (4×10^{-5}), 1150 (170), 146 (5). Accordingly, the line width for $D_2(\text{IV})$ and $D_{2d}(\text{II})$ shows a broad maximum around 125 and 150 K, respectively, (Figure 7). It is noteworthy that isomer $D_2(\text{II})$ also presents a low-lying level above its LUMO (Figure 3), albeit no such variation of its g -value.

Studies with room-temperature ESR show that upon warming up the anionic solutions, the ESR signals transformed into extremely thin signals (ca. 60 mG²⁶) with fine structure, widely varying in the number of lines from one isomer to another (Figure 8). Although, we do not have an explanation for such phenomenon at the moment, we feel important to make these

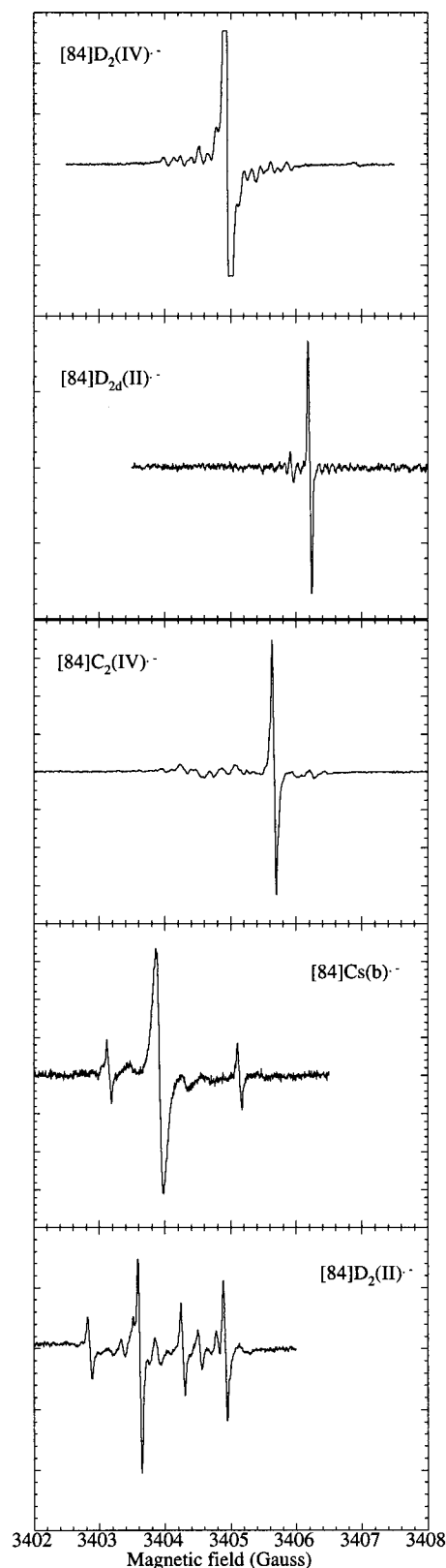


Figure 8. Room-temperature ESR solution spectra in benzonitrile. There is no spectrum for $D_{2d}(\text{I})$ due to lack of intensity at this temperature. The central line of $[84]D_2(\text{IV})^-$ is out of scale in order to reveal the fine structure.

spectra available to the community. More experienced ESR specialists might have an explanation readily available and, furthermore, these highly different spectra for each isomer could serve as an identification tool for further work, without requiring ¹³C NMR.

4. Conclusion

The electrochemical and ESR data presented constitute a fingerprint of six different chemical species, four of them having never been characterized before and thus add to the growing library of fullerene features. Identification of the C_2 isomer as $C_2(IV)$ is made by comparing calculations and electrochemical data. This $[84]C_2(IV)$ fullerene appears as a suitable candidate to obtain charge-transfer salts with TTF-based organic donors. Both $D_2(IV)$ and $D_{2d}(II)$ isomers exhibit dramatic variation of their ESR spectra with temperature which was interpreted as the population of a low-lying excited spin state. Finally, room-temperature solution ESR spectra of the isomeric radical-anions exhibit extremely narrow signals with a fine structure that might serve as a future identification tool.

Acknowledgment. This work was made possible through a French-Mexican cooperation program (action ECOS-ANUIES-SEP-CONACyT M96E01). J.A.A.B. and A.P. thank Dr. Juan Luis Peña for his support, H.S. thanks the JSPS Future Program for financial support, and T.J.S.D. thanks the Royal Society. This work was partially supported (G.E.S.) by NSF grant CHE-99821565.

Supporting Information Available: Supporting Information Available: Energy levels (BLYP/6-31G*) for C_{84} isomers $D_2(I)$, $D_2(II)$, $D_2(III)$, $D_2(IV)$, $D_{2d}(I)$, $D_{2d}(II)$, C_1 , $C_5(V)$, $C_2(I)$, $C_2(II)$, $C_2(III)$, $C_2(IV)$, $C_2(V)$. This material is available free of charge via the Internet at <http://pubs.acs.org>.

References and Notes

- (1) Kikuchi, K.; Nakahara, N.; Wakabayashi, T.; Suzuki, S.; Shiromaru, H.; Miyake, Y.; Saito, K.; Ikemoto, I.; Kainosho, M.; Achiba, Y. *Nature* **1992**, *357*, 142–145.
- (2) (a) Manolopoulos, D. E.; Fowler, P. W.; Taylor, R.; Kroto, H. W.; Walton, D. R. M. *J. Chem. Soc., Faraday Trans.* **1992**, *88*, 3117. (b) Taylor, R.; Langley, G. J.; Avent, A. G.; Dennis, T. J. S.; Kroto, H. W.; Walton, D. R. M. *J. Chem. Soc., Perkin Trans. 2* **1993**, 1029–1036.
- (3) Dennis, T. J. S.; Kai, T.; Tomiyama, T.; Shinohara, H. *Chem. Commun.* **1998**, 619–620.
- (4) Meier, M. S.; Guarr, T. F.; Selegue, J. P.; Vance, V. K. *J. Chem. Soc. Chem. Commun.* **1993**, 63–65.
- (5) Boulas, P.; Jones, M. T.; Kadish, K. M.; Ruoff, R. S.; Lorents, D. C.; Tse, D. S. *J. Am. Chem. Soc.* **1994**, *116*, 9393–9394. Boulas, P. L.; Jones, M. T.; Kadish, K. M.; Ruoff, R. S.; Lorents, D. C.; Tse, D. S. *J. Phys. Chem.* **1996**, *100*, 7573–7579.
- (6) Yang, Y.; Arias, F.; Echegoyen, L.; Chibante, L. P. F.; Flanagan, S.; Robertson, A.; Wilson, L. J. *J. Am. Chem. Soc.* **1995**, *117*, 7801–7804.
- (7) Azamar-Barrios, J. A.; Muñoz P. E.; Pénicaud, A. *J. Chem. Soc., Faraday Trans.* **1997**, *93*, 3119–3123.
- (8) Anderson, M. R.; Dorn, H. C.; Stevenson, S. A.; Dana, S. M. *J. Electroanal. Chem.* **1998**, *444*, 151–154.
- (9) Allen, K. M.; Dennis, T. J. S.; Rosseinsky, M. J.; Shinohara, H. *J. Am. Chem. Soc.* **1998**, *120*, 6681–6689.
- (10) Balch, A. L.; Ginwalla, A. S.; Lee, J. W.; Noll, B. C.; Olmstead, M. M. *J. Am. Chem. Soc.* **1994**, *116*, 2227–2228.
- (11) Margadonna, S.; Brown, C. M.; Dennis, T. J. S.; Lappas, A.; Pattison, P.; Prassides, K.; Shinohara, H. *Chem. Mater.* **1998**, *10*, 1741–1744.
- (12) Dennis, T. J. S.; Hulman, M.; Kuzmany, H.; Shinohara, H. *J. Phys. Chem. B* **2000**, *104*, 5411–5413.
- (13) Saunders, M.; Jiménez-Vásquez, H. A.; Cross, R. J.; Billups, W. E.; Gesenberg, C.; Gonzalez, A.; Luo, W.; Haddon, R. C.; Diederich, F.; Herrmann, A. *J. Am. Chem. Soc.* **1995**, *117*, 9305–9308.
- (14) Avent, A. G.; Dubois, D.; Penicaud, A.; Taylor, R. *J. Chem. Soc., Perkin Trans. 2* **1997**, 1907.
- (15) Dennis, T. J. S.; Kai, T.; Asato, K.; Tomiyama, T.; Shinohara, H.; Yoshida, T.; Kobayashi, Y.; Ishiwatari, H.; Miyake, Y.; Kikuchi, K.; Achiba, Y. *J. Phys. Chem. A* **1999**, *103*, 8747–8752.
- (16) Tagmatarchis, N.; Avent, A. G.; Prassides, K.; Dennis, T. J. S.; Shinohara, H. *Chem. Commun.* **1999**, 1023–1024.
- (17) Crassoux, J.; Rivera, J.; Fender, N. S.; Shu, L.; Echegoyen, L.; Thilgen, C.; Herrmann, A.; Diederich, F. *Angew. Chem., Int. Ed. Engl.* **1999**, *38*, 1613–1617.
- (18) Wheland, R. C. *J. Am. Chem. Soc.* **1976**, *98*, 3926–3930.
- (19) For the prototypical charge-transfer salt TTF-TCNQ, see Ferraris, J.; Cowan, D. O.; Walatka, V.; Perlstein, J. H. *J. Am. Chem. Soc.* **1973**, *95*, 948.
- (20) Dubois, D.; Moninot, G.; Kutner, W.; Jones, M. T.; Kadish, K. M. *J. Phys. Chem.* **1992**, *96*, 7137. Koh, W.; Dubois, D.; Kutner, W.; Jones, M. T.; Kadish, K. M. *J. Phys. Chem.* **1993**, *97*, 6871. Krishnan, V.; Moninot, G.; Dubois, D.; Kutner, W.; Kadish, K. M. *J. Electroanal. Chem.* **1993**, *356*, 93.
- (21) Gallagher, S. H.; Armstrong, R. S.; Lay, P. A.; Reed, C. A. *J. Phys. Chem.* **1995**, *99*, 5817–5825.
- (22) Yang, C. C.; Hwang, K. C. *J. Am. Chem. Soc.* **1996**, *118*, 4693–4698.
- (23) In Figure 4, parts a and c, entries have been included from ref 6 for $D_2(IV)$ and $D_{2d}(II)$. These values have been modified to take into account our different electrochemical setup. We have used as comparison the redox potentials of C_{76} as published in refs 6 and 25. The oxidation potential is the same within 10 mV but our reduction potential is ca. 100 mV more negative than that in ref 6. The values for Figure 4, parts a and c, have thus been modified by adding 100 mV to the values of ref 6, to have consistent data. It is important to stress that using unmodified data or even not using entries for $D_2(IV)$ and $D_{2d}(II)$ does not change the conclusion about $C_2(IV)$ assignment.
- (24) Kahn, O. *Molecular Magnetism*; VCH: New York, 1993; Chapter 4.
- (25) Azamar-Barrios, J. A.; Penicaud, A. In *Recent advances in the chemistry and physics of fullerenes and related materials*; Kadish, K. M., Ruoff, R. S., Eds.; The Electrochemical Society, Inc.; Pennington, NJ, 1997; Vol. 5, pp 54–57.
- (26) Note that this is very close to the manufacturer lower line width limit (35 mG); hence, it should be considered as an upper limit for the line width of C_{84} isomers.